Microstructure analysis of laboratory and in-situ compacted silts

Giacomo Russo [1,a], Andrea Rezza [1], Claudio Mancuso[2], Vincenzo Oliviero[2], Francesca D'Onza[3], Domenico Gallipoli[4] and Simon Wheeler[5]

[1]*Department of Civil and Mechanical Engineering, University of Cassino and Southern Lazio, Italy*
[2]*Department of Department of Civil, Architectural and Environmental Engineering, University of Naples Federico II, Italy*
[3] *Italian National Agency for the New Technologies, Energy and Sustainable Economic Development, ENEA, Italy*
[4] *Laboratoire SIAME, Université de Pau et des Pays de l'Adour, France*
[5] *School of Engineering, University of Glasgow, UK*

Abstract. The paper presents and discusses some results of an experimental research aimed at analysing the influence of compaction variables (w and energy) and method on the resulting microstructure of a compacted silty soil. In particular, the experimental data here discussed allow to compare the microstructure induced by different dynamic compaction techniques, comparing that characterising specimens obtained by two laboratory methods (Proctor standard and Harvard) and that of samples compacted in-situ during the construction of an embankment built for river regimentation purposes. Both undisturbed and disturbed samples have been retrieved from the embankment, the latter one with the purpose of collecting the soil subsequently used for laboratory compaction. Microstructural analyses (SEM, MIP) performed on laboratory and in-situ compacted samples evidenced a substantial similarity of the texture induced by the various compaction techniques, highlighting that laboratory compaction is suitable to provide soil samples representative of earth in-situ compacted soil.

1 Introduction

At the phenomenological scale of laboratory tests the experimental evidence highlights that the microstructure of compacted soils depends on water content and dry density adopted for the specimen preparation. In fact, it is well known that soil compacted wet of optimum, tends to have a homogenous texture, whereas those compacted on the dry side tends to exhibit a bimodal pore size distribution, referred to as 'double structure'[1, 2, 3, 4, 5], with two or more distinct classes of pore dimensions characterising the soil texture. Typically, there are two distinct classes of pores, the larger one characterising the inter-aggregate pore space and the smaller ones typical of the aggregates, thus named intra-aggregate pores [6, 7]. The distribution of the pore classes is likely to influence the idro-mechanical behaviour of the compacted soils.

In the paper some results on microstructural analyses on in-situ and laboratory compacted samples are reported. Some of the tested samples have been retrieved from an experimental embankment, 'identical' to the real embankments used for river regimentation purposes, built in order to evaluate the evolution of suction caused by soil-atmosphere and simulated flooding in real earth structure [8] . The embankment was constructed using the same compaction techniques adopted for service embankments using a fine-grained soil of medium plasticity taken from the floodplain. Other samples (from the same soil) have been compacted in the laboratory using the Proctor standard and the Harvard compaction techniques. All the above-mentioned group of samples have been subjected to an extensive testing program in order to characterise their hydro-mechanical behaviour and to laboratory tests to analyse their microstructure. These latter tests form the focus of the present paper and are based on mercury intrusion porosimetry (MIP) performed in order to obtain a quantitative description of the microstructure of soils and the evolution of the pore size distribution (PSD) after mechanical and hydraulic paths. MIP tests allowed the comparison of pore size distributions induced by different laboratory compaction procedures and initial water contents. Scanning electron microscopy (SEM) observations have been also performed to further investigate the compaction induced fabric of the mentioned classes of samples.

2 Material and experimental procedures

2.1 Alluvial silt

The soil is an alluvial sandy silt with relatively low clay fraction, as showed by the grain size distribution reported in Figure 1. The main physical properties of the soil are reported in Table 1. Overall the soil is classified as an inorganic silt of medium/high plasticity.

[a] Corresponding author: giarusso@unicas.it

Table 1. Physical properties of alluvial silt.

Specific gravity	Gs	2.75
Plastic limit	w_P	20
Liquid limit	w_L	37
Plasticity Index	PI	17

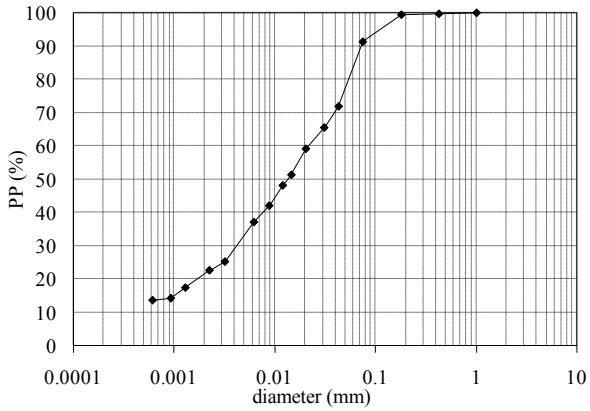

Figure 1. Grain size distribution of alluvial silt.

2.2 Compaction

The Standard Proctor compaction curve obtained for this soil by the ASTM D698-00a standard is reported in Figure 2, showing an optimum water content (w_{opt}) of 20.7% and a (maximum) dry density (γ_{dmax}) of 1.65 g/cm^3.

The analysis of the in situ undisturbed samples retrieved during the construction (here not reported) confirmed that soil construction of the embankment was performed in wet conditions [8], with water contents higher than the reference Proctor optimum. It is worth noting, however, that the data shown refer to samples retrieved from the embankment some years after its construction, thus the actual water content values are likely to be also influenced by wetting-drying cycles that the embankment itself underwent under service conditions. In order to reproduce initial conditions similar to the in-situ ones, it was decided to adopt the Harvard procedure [9] as it allows to obtain samples smaller of the Proctor ones with comparable physical properties.

As well known, the Harvard compaction apparatus consists in a small volume mould (62.4 cm^3) hold by an extension collar, a base and clamps. The tamper consists of a brass rod carrying a spring, with a wooden handle on one end. Springs of different stiffness are available to perform compaction. The soil is compacted in five layers under the load transferred by pushing down a selected number of times the handle, with the possibility of selecting the spring stiffness. The Harvard compaction procedure has been calibrated with the standard Proctor procedure following the ASTM D4609-01. A number of 35 pressures of the spring of stiffness 20 lb resulted in a dry density of the soil within the interval of ± 0.016 g/cm^3 of the Proctor standard maximum dry density at a w_{opt} = 20.7%, as requested by the ASTM procedure.

In Figure 2 the Harvard compaction curve is also reported and compared with the Proctor one. The initial state of the in-situ sample B is also shown together with some points (crosses) obtained by the Harvard compaction procedure.

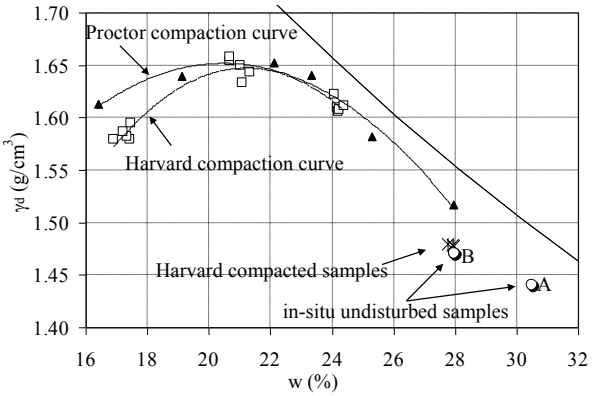

Figure 2. Standard Proctor compaction curve and undisturbed in-situ compacted samples.

2.3 Microstructure analyses

MIP tests were performed by a double chamber Micromeritics Autopore III apparatus. In the filling apparatus (dilatometer) the samples were outgassed under vacuum and then filled by mercury allowing the increase of absolute pressure up to the ambient one. Using the same unit the intrusion pressure was than raised up to approximately 200 kPa by means of compressed air. The detected entrance pore diameters ranges between 134 μm and 7.3 μm (approximately 0.01 MPa - 0.2 MPa for a mercury contact angle of 139°). After depressurisation to the ambient pressure, the samples were transferred to the high-pressure unit, where the mercury pressure was increased up to 205 MPa following a previously set intrusion program. At any intrusion step a time sufficient to observe a quasi-static penetration of mercury [10] was allowed. Corrections to the pore-size distribution due to the compressibility of the intrusion system were applied performing a blank test. The inner central region of each compacted sample was carefully cut in small pieces of approximately 1 – 2 g to obtain the MIP specimens. Sample dehydration requested before performing MIP analyses was obtained according to the freeze-drying method [11].

SEM analyses were performed on dehydrated samples in order to highlight their fabric.

3 Results

The cumulative intruded volume has been represented as a function of the entrance size of pores in terms of intruded void ratio e_{MIP}, defined as the ratio between the mercury intruded volume and the volume of solids. At the end of the intrusion stage, e_{MIP} can be directly compared to the reference void ratio of the sample e_0 determined in

a traditional way by measuring the volume and water content of the sample used for the MIP tests. The initial properties of the MIP samples considered in this paper are reported in Table 2.

Table 2. Physical properties of MIP samples.

Sample	w (%)	e_0	e_{MIP}
Proctor w_opt	20.00	0.674	0.378
Harvard w_opt	20.10	0.670	0.557
in situ_A	31.36	0.909	0.745
in situ_B	25.73	0.870	0.686
Harvard in situ	26.53	0.859	0.606

In Figure 3 a comparison between MIP tests on standard Proctor and Harvard compacted samples at optimum water content is reported, evidencing the similar texture of the specimen despite the different compaction techniques. In particular, Figure 3a shows a difference in the cumulated intrusion void ratios after the intrusion stage, with a higher intruded void ratio e_{MIP} for the Harvard sample, closer to the initial void ratio e0. Both the pore size distributions show (Figure 3b) a mono-modal curve, with the most frequent value of pore entrance size between 0.3 ÷ 0.4 μm.

In Figure 4 some SEM images of the two samples are reported, confirming the similarity of their microstructural organization, independently on the compaction method. The occurrence of slightly larger pores can be observed for the Harvard sample (Figure 4b). As a result, the similar features induced by different compaction techniques at optimum water content confirmed the suitability of the Harvard technique for preparing MIP samples comparable with the Proctor standard one.

Figure 5 reports the results of the MIP tests performed on the in-situ compacted samples A and B (see Figure 2) and the Harvard one prepared at the same initial water content of B. Comparing the cumulative intruded void ratio of the in-situ samples (Figure 5a), it can be observed that for the sample A the intruded void ratio is higher than the sample B, as expected from its higher initial water content and lower dry density. The cumulative intruded volume of the Harvard sample compacted at in-situ water content is closer to the B in situ samples, as expected for the initial state of the samples. The intruded void ratio at the end of the intrusion stage e_{MIP} is lower than the initial void ratio e_0 of the samples, highlighting a similar degree of not intruded porosity of the three samples.

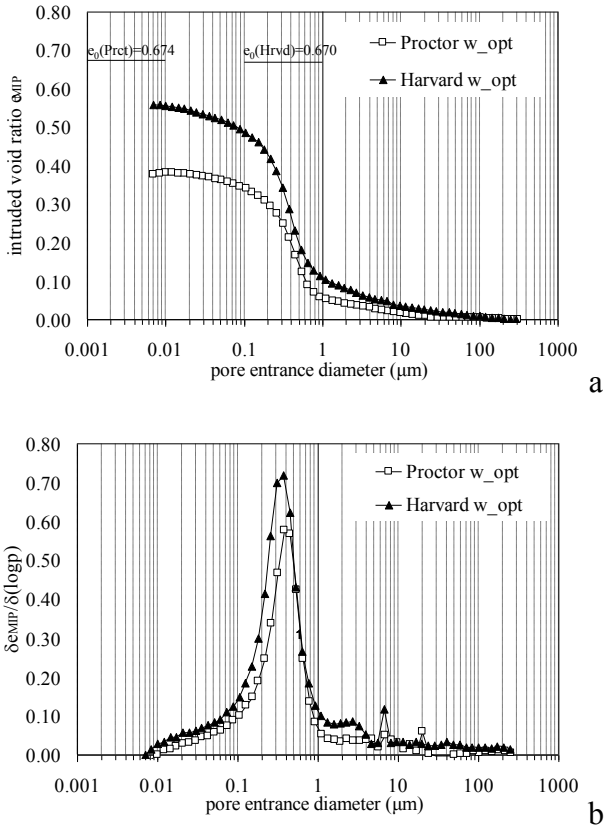

Figure 3. MIP results on Standard Proctor and Harvard compacted samples at optimum water content. a) intruded void ratio, b) pore size density function.

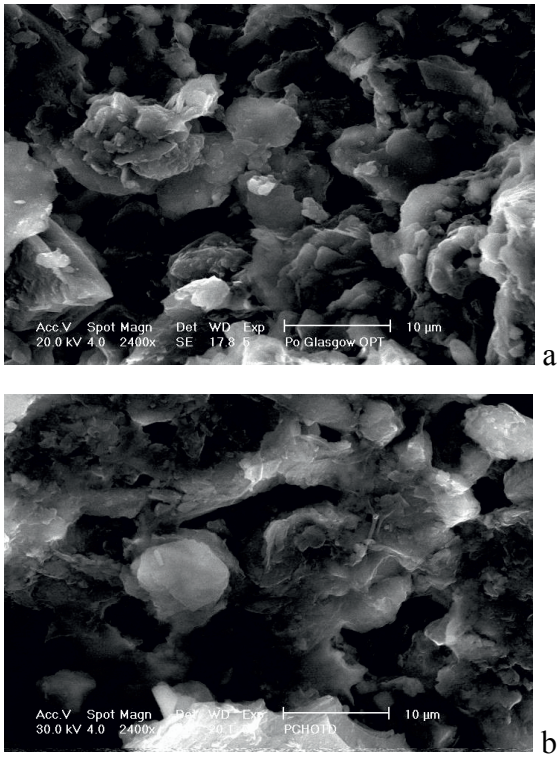

Figure 4. SEM analyses on a) Standard Proctor and b) Harvard compacted samples.

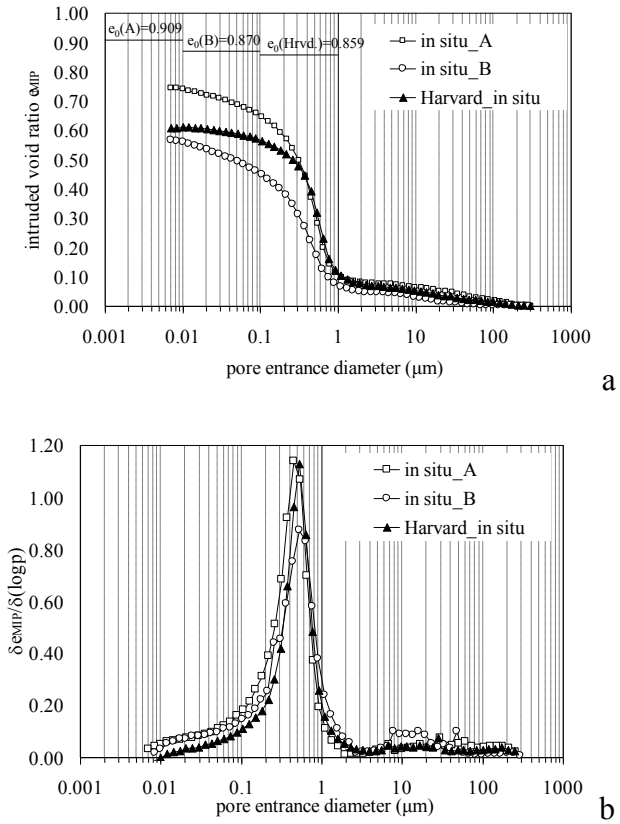

Figure 5. MIP results on in-situ samples A and B and Harvard compacted sample at in-situ water content. a) intruded void ratio, b) pore size density function.

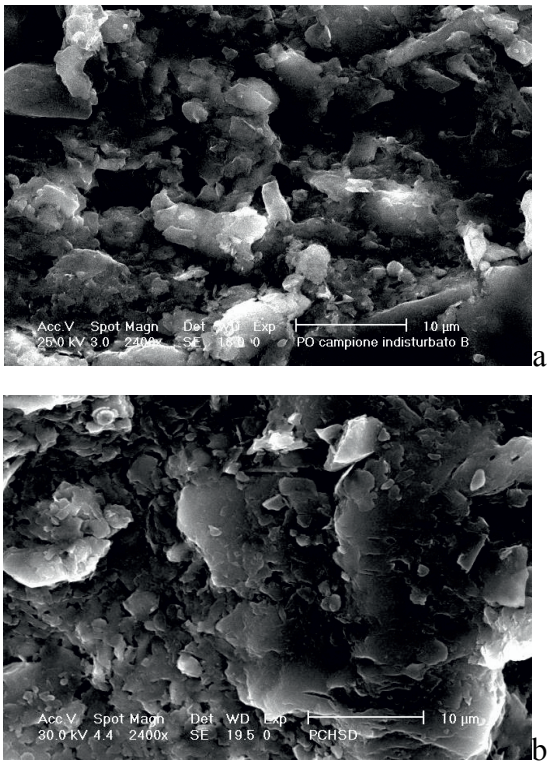

Figure 6. SEM analyses a) on in-situ sample B and b) Harvard compacted sample at in-situ water content.

The frequency of pore entrance diameters is very similar for both the in-situ and laboratory compacted samples. The mono-modal curves of the pore size density functions showed in Figure 5b highlight a close correspondence, with the most frequent entrance pore diameter in the range 0.4–0.6 μm. A slighter difference can be found in the frequency of smaller pores (pore entrance diameter < 0.4 μm), which is systematically higher for the in situ undisturbed samples A and B with respect to the Harvard sample.

Finally, Figure 6 shows the SEM images of the in-situ B sample and Harvard one. The aggregated fabric of the two samples are quite similar apart for the detection of pores of relatively large entrance size for the sample B in the range between 1 μm and 10 μm (consistent with the slightly higher frequency evidenced by the MIP results in the same range), and an apparent less frequency of small pores inside the aggregates characterizing the fabric of the Harvard sample.

4 Conclusions

The paper reports some results of a joined research program between several institutions (see the heading of the paper) on the hydro-mechanical behaviour of a compacted alluvial silt. The results of MIP tests and SEM images from undisturbed samples taken from an experimental embankment and specimens obtained in the laboratory by different compaction techniques are presented and discussed to analyse possible effects of the compaction variables (w, energy) and method on the microstructure of the resulting soils. To this end, the microstructure of Proctor standard, Harvard and in-situ undisturbed samples has been analysed and compared. The comparison of Proctor standard and Harvard specimens at the optimum water content and density highlighted very similar soil fabrics, suggesting that the compaction technique does not play such an important role on the final texture taken on by compacted soils. The comparison between the microstructure of in situ undisturbed samples and Harvard ones compacted on the wet side at very similar water content and dry density also highlighted significant common features of the microstructure. In both the above mentioned cases, the results seem to confirm the validity of using laboratory compacted sample as reference for the analysis of the hydro-mechanical behaviour of soils used as construction materials.

Acknowledgments

The contribution of the European Commission via the Career Integration Grant SAFES (Service Assessment and Failure of Earth Structures), contract n. PCIG09-GA-2011-293727, is gratefully acknowledged.

References

1. Barden L., Sides G.R., J. Soil Found. An. 96:1171–1200, (1970).
2. Sridharan A, Altaschaeffl A.G., Diamond S. J.S.Mech.&Found.Div. ASCE, 97, 771–787, (1971)
3. Collins K, McGown A. Géotech. 24:223–254, (1974)
4. Alonso E.E., Gens A., Hight D.W. Proc. 9th ECSMFE, 5.1–5.60, (1987)
5. Cuisinier, O. & Laloui, L. Int. J. Num. &An. Meth. in Geomech., 28, 483-499 (2004)
6. Delage, P., Audiguier, M., Cui, Y.J, and Howat, D.. Can. Geotech. J. 33: 150-158, (1996)
7. Romero, E., A. Gens & A. Lloret. Eng. Geol. 54: 117-127 (1999)
8. Calabresi G., Colleselli F., Danese D., Giani G., Mancuso C., Montrasio L., Nocilla A., Pagano L., Reali E., Sciotti A. Can. Geotech. J. 50: 947–960 (2013)
9. Wilson, S., D. Eng.News Rec., (1950)
10. Romero, E., Simms, P. Geotech.l and Geol. Eng. 26:705-727, (2008).
11. Delage, P., Pellerin, F.M. Cl. Min., 19: 151-160, (1984).